

## A Coordinated LVRT Control for a PMSG Wind Turbine

Chunghun Kim\* Yonghao Gui\*\*,\* Chung Choo Chung†\*

\* Dept. of Electrical Engineering, Hanyang University, Seoul, Korea

(e-mail: freidee@hanyang.ac.kr; cchung@hanyang.ac.kr)

\*\* Dept. of Energy Technology, Aalborg University, 9220 Aalborg, Denmark.

(e-mail: yog@et.aau.dk)

**Abstract:** This paper proposes a coordinated controller for a permanent-magnet synchronous generator wind turbine to enhance its low voltage ride through capability. In the proposed method, both rotor side and grid side converters are cooperatively controlled to regulate the DC link voltage during the grid fault. Moreover, at the fault clearance, the grid side converter produces the previous power value which is the maximum power in normal operation. It prevents excessive power production at the fault clearance in order to reduce the rotor load. From the proposed method, better transient response of the DC link voltage could be obtained with less rotor acceleration. We validated the proposed method using MATLAB/Simulink SimPowerSystems and compared the performances of with and without the coordinated control.

© 2017, IFAC (International Federation of Automatic Control) Hosting by Elsevier Ltd. All rights reserved.

**Keywords:** Coordinated controller, Sliding mode control, Low voltage ride through

### • Nomenclature

- PMSG : Permanent magnet synchronous generator
- WPS : Wind power system
- DFIG : Doubly-fed induction generator
- MPPT : Maximum power point tracking
- FRT : Fault ride through
- LVRT : Low voltage ride through
- WT : Wind turbine
- SMC : Sliding mode control
- RSC : Rotor-side converter
- GSC : Grid-side converter
- PCC : Point of common coupling
- PI : Proportional-integral

### 1. INTRODUCTION

The wind power generation is taken notice as one of the most growing renewable energy in terms of its costs and benefits. PMSG in WPS has many advantages in comparison with the DFIG wind systems. These advantages are high power density, no gearbox, simple control method and high precision, whereas PMSG needs to high initial installation costs Polinder et al. (2006); Chinchilla et al. (2006) because of the use of permanent magnet. When the penetration level is not significant, WPS only has a control objective of MPPT control which could be achieved by model based or model free methods Kim et al. (2017). As wind energy penetration level in the electrical power systems increases, many grid codes requires that wind power systems remain connected to the grid during the event of network disturbances Tsili and Papathanassiou (2009). Otherwise, the sudden disconnections of wind turbines when the grid faults could result in cascaded generation outage. For this reason, grid codes describe that large wind power plants are required to remain connected to the grid when voltage dips down to a

\* †: Corresponding Author

This work was supported by the Korea Electric Power Co., Ltd.[KEPCO].

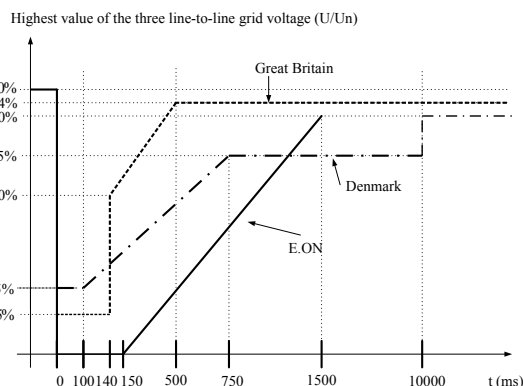


Fig. 1. Limit curves for the voltage to allow generator disconnection Tsili and Papathanassiou (2009).

certain percentage of the nominal voltage (0% in some cases) for a specified duration Tsili and Papathanassiou (2009). And these specific requirements are decided considering the power system characteristics. Such requirements are known as FRT or LVRT requirements for wind power plants and many countries think it as one of the most important thing for grid integration to the power system. Grid codes describe voltage characteristics against time, denoting the minimum required time to be connected during the dips of the system voltage Tsili and Papathanassiou (2009). Fig. 1 shows the LVRT requirements of Germany(E.ON), Great Britain, and Denmark Tsili and Papathanassiou (2009) and each countries have substantial wind power penetration level.

To satisfy these requirements during faults, several methods for PMSG WT were proposed Saccomando et al. (2002); Mullane et al. (2005); Matas et al. (2008); Conroy and Watson (2007); Kim et al. (2012); Alepuz et al. (2013); Wang et al. (2010); Gui et al. (2015, 2016). For a PMSG WT system, the effects of voltage dips on the performance of the controller under

unbalanced conditions were studied Saccomando et al. (2002). The PI controller of the DC link using current feedforward was proposed without considering the controller impact on the converter currents. A feedback linearization nonlinear controller was proposed for the grid-side converter of PMSG Mullane et al. (2005). This controller was designed to improve the behavior of the conventional linear current controllers for voltage sag, keeping the current levels within the limit. However, it was too difficult to implement, because it involves a number of terms, divisions and required sensing of the DC link currents or its time derivative. To avoid these problems, the feedback linearization was applied through a SMC approach Matas et al. (2008). To implement this method, the control algorithm is conducted in the grid-side converter to regulate the DC link voltage considering current. For the PMSG WT system, the combined control scheme of the braking resistor, the pitch angle, and the converter control was designed to protect the WT and allow it to remain connected to the grid Conroy and Watson (2007). Some research results have been suggested applying the DC link voltage control strategies in the generator-side converter instead of the grid-side converter since it is hard to control the grid-side converter during the network faults. Through this strategy, the DC link voltage can be regulated as a constant by increasing the generator speed from rotor-side control during the grid voltage sag Kim et al. (2012); Alepuz et al. (2013). For the generator-side converter, a feedback linearization controller was proposed Kim et al. (2012). There are some other methods using the additional device for the LVRT. The vanadium redox flow battery based energy storage system is added at the DC link bus to regulate DC link voltage Wang et al. (2010). The passivity based control method with and without considering a DC chopper control was proposed to improve LVRT capability Gui et al. (2015, 2016).

We propose the coordinated LVRT control which modifies both RSC and GSC to regulate the DC link voltage. To obtain the better performance of DC link voltage regulation, we use quasi-continuous SMC method in RSC control and GSC cooperatively regulates the DC link voltage during the fault. i.e., GSC changes its control scheme between normal and fault durations. During normal operation, the GSC is controlled for tracking the MPPT point. When there is voltage dips in the grid, GSC switches its control mode to regulate the DC link voltage cooperative to the RSC. During the fault ride through period, the rotor speed increases storing the kinetic energy in its inertia, simultaneously. Consequently, WT is controlled within derating region to reduce its power during the ride through period. The behavior of derating control was studied and its input to state stability was illustrated in Buckspan et al. (2013). And we also modifies the after fault behavior of the GSC to produce the previous MPPT power. From this modification, the rotor load was reduced after the fault duration and it is more helpful for grid stability by producing the converged power right after the fault clearance. We compared the performance of the DC link regulation with previously proposed SMC method without coordinated control. The proposed method has less peak value in DC link voltage during the fault and more fast convergence.

## 2. PMSG WIND POWER SYSTEMS

In this section, we briefly describe the modeling of the RSC, GSC and the DC link voltage.

### 2.1 Modeling of Rotor Side Converter

To obtain the mechanical power from a WT, the power coefficient,  $C_p$ , should be defined composed of tip speed ratio,  $\lambda$  and pitch angle,  $\beta$  Conroy and Watson (2007).

$$P_t = \frac{1}{2} \rho A C_p(\lambda, \beta) v_{wind}^3, \quad (1)$$

$$\lambda = \frac{\omega_m R}{v_{wind}},$$

where  $\rho$  is the air density,  $A$  is the blade swept area and  $C_p$  is the power coefficient which is a function of pitch angle,  $\beta$ , and the tip speed ratio,  $\lambda$ .  $v_{wind}$  is the wind velocity. The power coefficient is the ratio of electricity produced by WT to the total energy available in that wind speed and theoretical limit of this value is 0.5926. The practical value is less than this limit because of the loss of the mechanical systems in WT. To analyze electrical parts of the PMSG, we use the equations which are the voltage, current equations of PMSG and electrical and mechanical torque as introduced in Alepuz et al. (2013).

$$v_{dg} = R_s i_{dg} + L_s \frac{di_{dg}}{dt} - \omega_s L_s i_{qg},$$

$$v_{qg} = R_s i_{qg} + L_s \frac{di_{qg}}{dt} + \omega_s L_s i_{dg} + \omega_s \lambda_f,$$

$$T_e = \frac{3}{2} p \lambda_f i_{qg},$$

$$T_m - T_e = J \frac{d\omega_m}{dt}, \quad (2)$$

where,  $v_{dg}$ ,  $v_{qg}$  are stator voltages,  $i_{dg}$ ,  $i_{qg}$  are stator currents.  $L_s$  is the stator inductance,  $R_s$  is the stator resistance and  $\omega_s$  is the rotor flux electrical speed.  $\omega_m$  is the generator mechanical speed,  $\lambda_f$  is the rotor flux and  $p$  is the machine pole pairs.  $T_e$  is the electromagnetic torque,  $T_m$  is mechanical torque which could be obtained from the mechanical power.  $J$  is the inertia of rotor. By using  $T_e$ ,  $T_m$  and  $J$ , the rotor speed could be decided according to above equations. We use the surface mounted PMSG which has same d-axes and q-axes inductance. Thus, Reluctance torque which is occurred by difference between these inductances does not exist. Hence the electromagnetic torque could be described as (2).

### 2.2 Modeling of Grid Side Converter

The dynamics of the GSC in rotating frame is given by Haque et al. (2008),

$$v_d = v_{id} - R i_d - L \frac{di_d}{dt} + \omega L i_q,$$

$$v_q = v_{iq} - R i_q - L \frac{di_q}{dt} + \omega L i_d, \quad (3)$$

where  $L$  is the grid inductance,  $R$  is the grid resistance.  $v_d$  and  $v_q$  are d and q axis grid voltages.  $i_d$ ,  $i_q$  are d and q axis grid currents.  $v_{id}$ ,  $v_{iq}$  are d and q axis voltages of the converter, respectively. In rotating reference frame, we assumed that d-axis of rotating reference frame is aligned with vector of grid voltage. Therefore, the active and reactive powers to the grid can be described as Haque et al. (2008),

$$P_{grid} = \frac{3}{2} v_d i_d,$$

$$Q_{grid} = \frac{3}{2} v_d i_q. \quad (4)$$

We can find out that the active and reactive powers to the grid are controlled by  $i_d$ ,  $i_q$ , respectively.

### 2.3 DC Link Voltage

The DC link voltage could be obtained from the difference between generator side and grid side power flow Kim et al. (2012),

$$P_c = CV_{dc} \frac{dV_{dc}}{dt} = P_g - P_{grid}, \quad (5)$$

where  $P_g$  is the generator power,  $P_{grid}$  is the grid power and  $P_c$  is the DC link capacitor power.  $V_{dc}$  is the DC link voltage, and  $C$  is the DC link capacitor. It is the nonlinear equation since the DC link voltage and its derivatives are multiplied.

## 3. CONTROL SYSTEM

In this section, we illustrate the control algorithms for the RSC and GSC. We use the quasi-continuous SMC controller in the RSC for DC link voltage regulation. And unlike to previous works, we modify the GSC controller to cooperatively regulate the DC link voltage during the fault. In normal operation, the GSC is controlled to track the MPPT set point. Moreover, we set the GSC power set point as the previously produced MPPT power at the fault clearing phase. It is more beneficial to reduce the rotor load and to the grid since it produces set point power to the grid.

### 3.1 Rotor-Side Converter Control

We describe a RSC controller applied the SMC method to regulate the DC link voltage. Since the SMC method has a chattering problem we use the quasi-continuous algorithm in this SMC formulation. The controller is known as quasi-continuous algorithm if it can be redefined according to continuity everywhere except the sliding manifold ( $s = 0$ ). In practice, due to disturbances and noise, the trajectory does not hit the sliding manifold in normal case. Therefore, the control practically remains continuous function all the time. From this scheme, the chattering could be significantly reduced Levant (2012). For this reason, we use quasi-continuous SMC to regulate the DC link voltage in RSC control. To achieve this control objective, a tracking error is defined as follows.

$$e = V_{dc}^* - V_{dc}. \quad (6)$$

where  $e$  is the DC link voltage error and  $V_{dc}^*$  is the DC voltage reference. The sliding surface is defined as (15) for regulating the DC link voltage.

$$s = k_1 e + k_2 \int e, \quad (7)$$

$k_1$  and  $k_2$  are the controller gains. By differentiating the sliding surface, we could obtain the following equation.

$$\begin{aligned} \dot{s} &= k_1 \dot{e} + k_2 e, \\ &= \frac{k_1}{CV_{dc}} P_{grid} - \frac{k_1}{CV_{dc}} u + k_2 e. \end{aligned} \quad (8)$$

From (8), the equivalent control is obtained by,

$$\begin{aligned} 0 &= \frac{k_1}{CV_{dc}} P_{grid} - \frac{k_1}{CV_{dc}} u + k_2 e, \\ \Rightarrow u_{eq} &= P_{grid} + \frac{k_2 C}{k_1} e V_{dc}. \end{aligned} \quad (9)$$

**Proposition 1.** Consider the dynamic system (5), if taking a control law with (9) as

$$u = u_{eq} + \alpha \frac{\dot{s} + \beta |s|^{\frac{1}{2}} \text{sat}(\frac{s}{\epsilon})}{k_1 (|\dot{s}| + \beta |s|^{\frac{1}{2}})} \quad (\alpha > 0, \beta > 0), \quad (10)$$

where

$$\text{sat}\left(\frac{s}{\epsilon}\right) = \begin{cases} \frac{s}{\epsilon}, & \text{if } |s| \leq |\epsilon| \\ \frac{s}{|s|}, & \text{if } |s| > |\epsilon| \end{cases},$$

and  $\epsilon$  is a positive constant, then the system trajectory reaches the boundary layer of the manifold in finite time.  $\diamond$

**Proof:** Lyapunov function candidate could be used as,

$$V = \frac{1}{2} s^2. \quad (11)$$

The derivative of this Lyapunov function candidate with respect to time is

$$\begin{aligned} \dot{V} &= s\dot{s}, \\ &= s \left( \frac{k_1}{CV_{dc}} P_{grid} - \frac{k_1}{CV_{dc}} u + k_2 e \right). \end{aligned} \quad (12)$$

If taking a control law as (10), then (12) yields

$$\dot{V} = s\dot{s} = \begin{cases} -\frac{\alpha\beta|s|^{\frac{1}{2}}s^2}{\epsilon CV_{dc}(|\dot{s}| + \beta|s|^{\frac{1}{2}}) + \alpha}, & \text{if } |s| \leq |\epsilon|, \\ -\frac{\alpha\beta|s|^{\frac{3}{2}}}{CV_{dc}(|\dot{s}| + \beta|s|^{\frac{1}{2}}) + \alpha}, & \text{if } |s| > |\epsilon|. \end{cases} \quad (13)$$

If we use control parameters satisfying  $\alpha > 0$  and  $\beta > 0$ , it follows  $\dot{V} < 0$  when  $s \neq 0$ . Therefore, the system trajectory reaches the boundary layer of the manifold in finite time.  $\diamond$

### 3.2 Grid-Side Converter Control

In normal operation, the objective of the GSC control is the MPPT. However, In this paper, we change the control algorithm of the GSC during fault.

$$\begin{aligned} P_t &= \frac{1}{2} \rho A C_{pmax} \left( \frac{\omega_m R}{\lambda_{opt}} \right)^3 = K_{opt} \omega_m^3, \\ P_{grid}^* &= \begin{cases} K_{opt} \omega_m^3, & \text{if normal operation,} \\ P_{LVRT}, & \text{if grid voltage sag.} \end{cases} \end{aligned} \quad (14)$$

where,

$$P_{LVRT} = k_1 e + k_2 \int e. \quad (15)$$

If we assumed the electrical and mechanical losses are neglected, the MPPT control of the PMSG WT could be achieved by denoting the GSC power reference as in (14). The balance between the mechanical power and the electrical power makes it possible to track the maximum power from this GSC power reference. That is, since the RSC is controlled to regulate the DC link voltage, it is controlled to track the GSC power reference which results in the rotor speed variation according to the power balance. Eventually, the rotor speed tracks the rotor speed of MPPT which is the balancing point from this process. On the other hand, when the grid voltage sags, the generator provides the active power continuously but the power delivered to grid is decrease. Then, if the GSC does not operate any control action to regulate the DC link voltage during the grid voltage sag, the DC link voltage changes because of power imbalance between the generator and the grid. Since the one of the most important thing for the LVRT control is the DC link regulation which affect the converter control performance, we propose that the GSC is controlled to cooperatively regulate the DC link voltage during faults as described in (14) when the grid voltage sag. During this fault ride through behavior, the rotor speed increases storing the kinetic energy in its inertia simultaneously. Consequently, WT is controlled within derating region to reduce its power during the ride through period. The stability of derating control has been studied and its input to state stability has been proved in Bucksan et al. (2013).

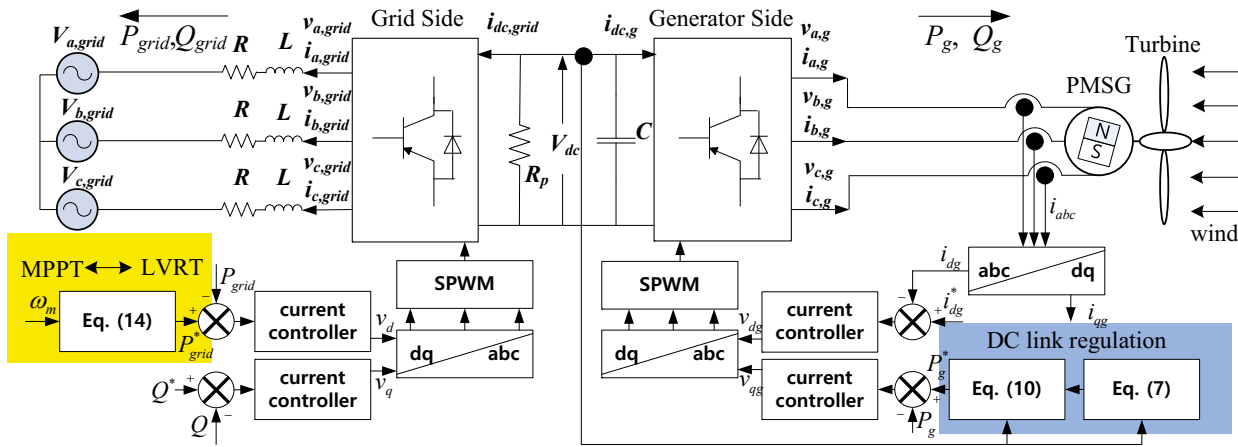


Fig. 2. Overall control block diagram of the generator and grid side converter

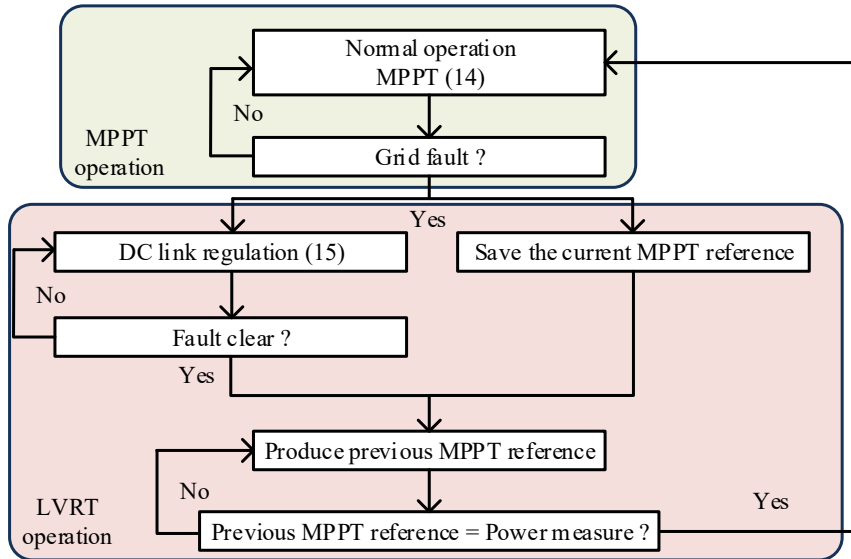


Fig. 3. Flow chart of the GSC switching operations of the normal and fault operations

Moreover, we designate the power production value at the fault clearance as the pre-fault MPPT value. From this process at the fault clearance, the excessive rotor load which occurs when the MPPT operation is activated right after the fault clearance according to (14) could be avoided. The proposed control block diagram for the system is shown in Fig. 2. And the detailed control flow chart of switch operation is illustrated in Fig. 3.

#### 4. SIMULATION RESULT

To validate the performance of the proposed algorithm, MATLAB/Simulink, SimPowerSystems was used for a 1.5 MW PMSG WT system connected to the grid. We simulated the voltage sag conditions with different voltage levels in the PCC and the parameters of the WT are denoted in Table. 1.

Firstly, we compared the LVRT performance of the proposed method with previously introduced SMC control without coordinated control of the GSC for the DC link voltage regulation. We set the 70% voltage sag in the grid voltage from 1s to 1.625s so that the fault duration is 0.625s. As shown in Fig. 4, the proposed method produces larger power output to the

grid during the fault than the previous method. And after the

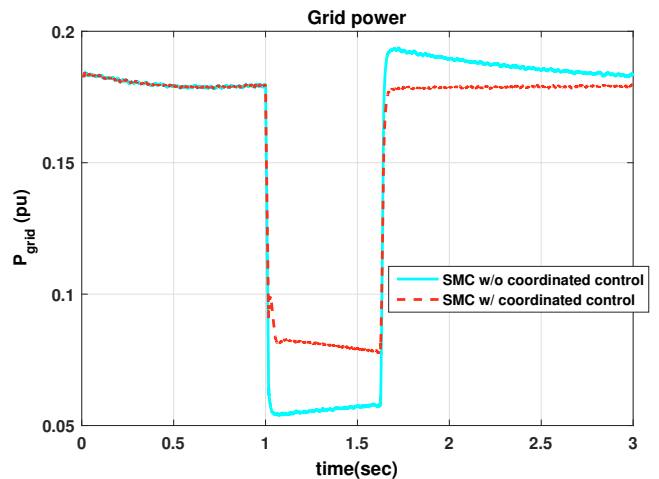


Fig. 4. Grid power performance for three-phase balanced voltage sag (70%).

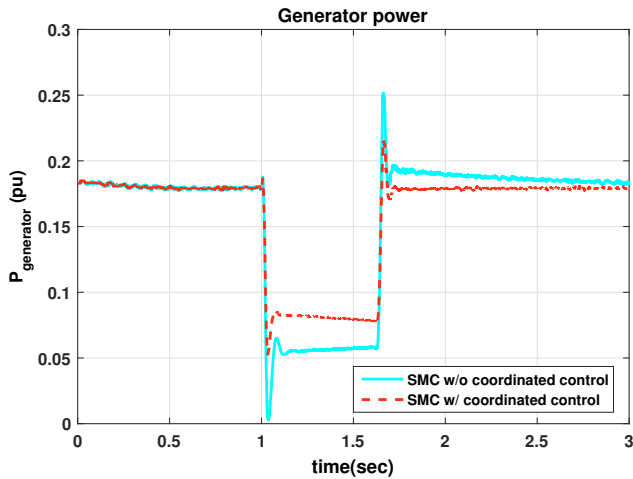


Fig. 5. Generator power performance for three-phase balanced voltage sag (70%).

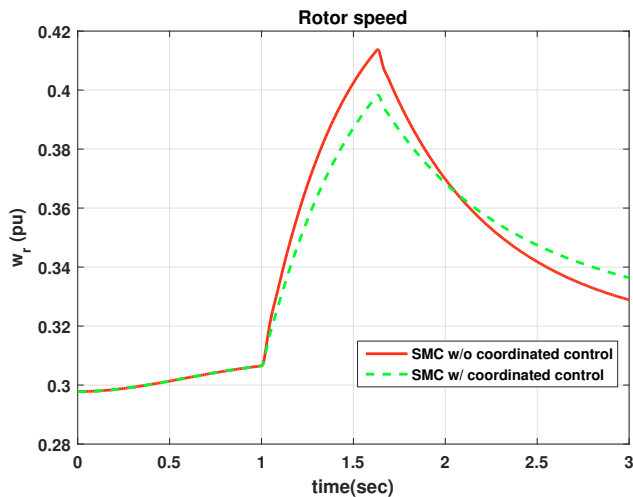


Fig. 6. Generator speed performance for balanced voltage sag (70%).

Table 1. System parameters used in simulation

Parameter	Value	Unit
Rated Power	1.5	MW
Wind speed	7	m/s
Max. power coeff.	0.44	
Optimal tip speed ratio	10.5	
Blade radius	33.05	m
Air density	1.225	kg/m <sup>3</sup>

fault, the proposed method produce the pre-fault power output to avoid the excessive grid power output according to the MPPT control. Fig. 5 describes the generator power output. From this figure, we can find out that more overshoot in the previous method when the fault is occurred and cleared. After the fault, the RSC produces excessive power according to the MPPT power reference and which forces the rotor speed to be reduced to the value for the MPPT. However, it results in excessive load to rotor due to the extreme ramp as shown in Fig. 6. Moreover, it is more helpful to the grid that the output power from the WT converge to the MPPT value more rapidly. From these perspectives, the proposed method is more

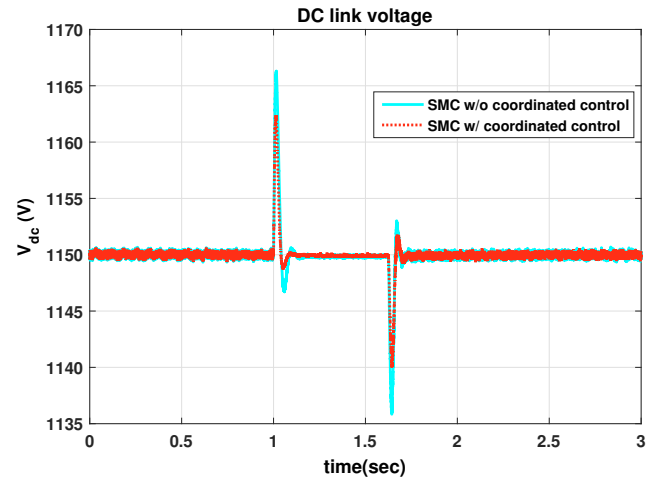


Fig. 7. DC link voltage regulation performance for balanced voltage sag (70%) for SMC w/o and w/ coordinated control.

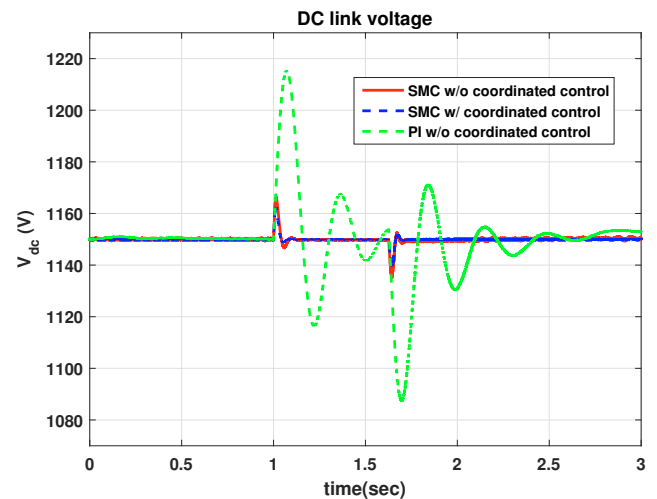
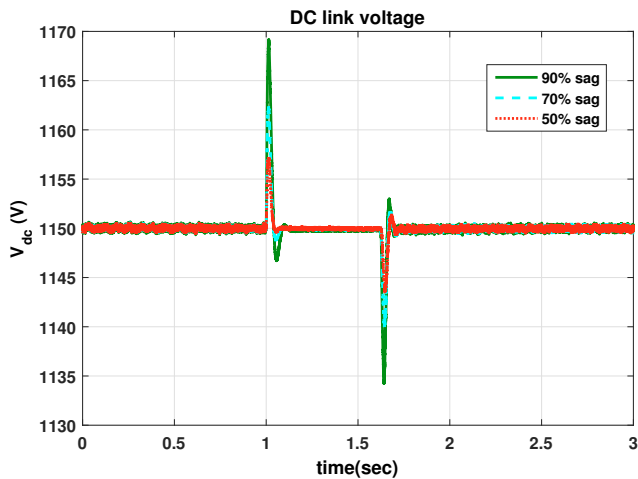
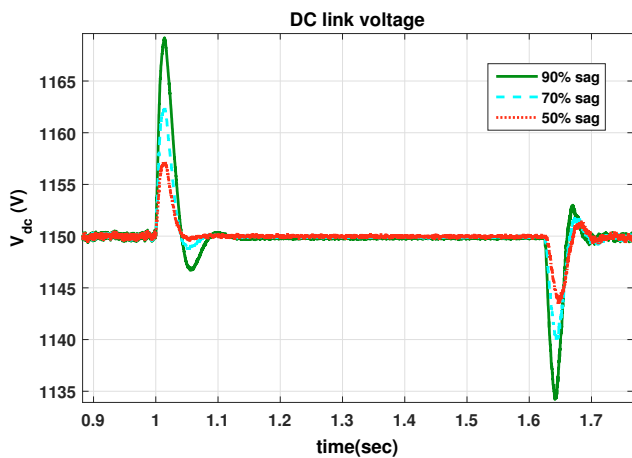


Fig. 8. Comparison of the DC link voltage regulation performance for balanced voltage sag (70%) for PI control and SMC w/o and w/ coordinated control.

helpful to the grid during fault since it produces MPPT set point power right after the fault clearance and does not cause excessive load to rotor. Fig. 7 describes the performance of DC voltage regulation. From this figure, the better performance could be obtained from the proposed method by changing the set point power properly when the fault occurs and clears. After the grid voltage sag clearance, the grid power reference recovers optimal power thus the grid and the generator power are recovered. The better transient response is observed under the SMC method with quasi-continuous algorithm because of nonlinear relationship between the DC link voltage and the generator power. Fig. 6 shows generator speed variation. The proposed method has less overshoot and ripple in the DC link voltage. It is reasonable since the proposed method has less overshoot and short convergence time in grid and generator side power production. Previous method has better performance of regulating the DC link voltage by modifying the RSC control with SMC control as shown in Fig. 8. Further improvement is achieved from the proposed method by adopting coordinated control of the GSC control of DC link regulation during fault.



(a) 50%(dotted red), 70%(dotted green), 90%(blue line)



(b) Magnified plot of Fig. 8(a)

Fig. 9. DC link voltage performance for various voltage sag w/ coordinated control.

We further investigate the various performance according to the different voltage sag levels. Fig. 9 describes the performance of different voltage sags as 50%, 70% and 90%. This figure illustrates that the less the voltage sags, the less peak in the DC link voltage.

## 5. CONCLUSIONS

We proposed the coordinated LVRT control which modifies both RSC and GSC to enhance the regulation of the DC link voltage. For this, we use the quasi-continuous SMC method in RSC and coordinated control in GSC by changing the operation during the fault. During normal operation, the GSC is controlled for tracking the MPPT point. When there is voltage dips in the grid, the GSC is controlled to regulate the DC link voltage cooperative to the RSC. And we also modifies the GSC output power reference as the previous MPPT power. From this modification, the rotor load was reduced after the fault duration by avoiding excessive power production in the GSC. From this control scheme, moreover, it could be more helpful to grid stabilization by producing the converged power right after the fault clearance. We compared the performance of the DC link regulation with previously proposed SMC method without

coordinated control. The proposed method has less peak value in DC link voltage during the fault and more fast convergence.

## REFERENCES

- Alepuz, S., Calle, A., Busquets-Monge, S., Kouro, S., and Wu, B. (2013). Use of stored energy in PMSG rotor inertia for low-voltage ride-through in back-to-back NPC converter-based wind power systems. *IEEE Trans. Ind. Electron.*, 60(5), 1787–1796.
- Buckspan, A., Pao, L., Aho, J., and Fleming, P. (2013). Stability analysis of a wind turbine active power control system. In *2013 American Control Conference*, 1418–1423. IEEE.
- Chinchilla, M., Arnaltes, S., and Burgos, J.C. (2006). Control of permanent-magnet generators applied to variable-speed wind-energy systems connected to the grid. *IEEE Trans. Energy Convers.*, 21(1), 130–135.
- Conroy, J.F. and Watson, R. (2007). Low-voltage ride-through of a full converter wind turbine with permanent magnet generator. *IET Renewable Power Generation*, 1(3), 182–189.
- Gui, Y., Kim, C., and Chung, C.C. (2015). Nonlinear control for PMSG wind turbine via port-controlled Hamiltonian system. In *Proc. IEEE PowerTech. Eindhoven*, 1–6.
- Gui, Y., Kim, C., and Chung, C.C. (2016). Improved low-voltage ride through capability for pmsg wind turbine based on port-controlled hamiltonian system. *International Journal of Control, Automation and Systems*, 14(5), 1195–1204.
- Haque, M.E., Negnevitsky, M., and Muttaqi, K. (2008). A novel control strategy for a variable speed wind turbine with a permanent magnet synchronous generator. In *Proc. IEEE. Ind. Appl. Soc. Annu. Meeting*, 1–8.
- Kim, C., Gui, Y., and Chung, C.C. (2017). Maximum power point tracking of a wind power plant with predictive gradient ascent method. *IEEE Transactions on Sustainable Energy*, 8(2), 685–694.
- Kim, K.H., Jeung, Y.C., Lee, D.C., and Kim, H.G. (2012). LVRT scheme of PMSG wind power systems based on feedback linearization. *IEEE Trans. Power Electron.*, 27(5), 2376–2384.
- Levant, A. (2012). Finite-time stability and high relative degrees in sliding-mode control. 59–92. Springer.
- Matas, J., Castilla, M., Guerrero, J.M., Garcia de Vicuna, L., and Miret, J. (2008). Feedback linearization of direct-drive synchronous wind-turbines via a sliding mode approach. *IEEE Trans. Power Electron.*, 23(3), 1093–1103.
- Mullane, A., Lightbody, G., and Yacamini, R. (2005). Wind-turbine fault ride-through enhancement. *IEEE Trans. Power Syst.*, 20(4), 1929–1937.
- Polinder, H., Van der Pijl, F.F., Vilder, D., Tavner, P.J., et al. (2006). Comparison of direct-drive and geared generator concepts for wind turbines. *IEEE Trans. Energy Convers.*, 21(3), 725–733.
- Saccomando, G., Svensson, J., and Sannino, A. (2002). Improving voltage disturbance rejection for variable-speed wind turbines. *IEEE Trans. Energy Convers.*, 17(3), 422–428.
- Tsili, M. and Papathanassiou, S. (2009). A review of grid code technical requirements for wind farms. *IET Renewable Power Generation*, 3(3), 308–332.
- Wang, W., Ge, B., Bi, D., Qin, M., and Liu, W. (2010). Energy storage based LVRT and stabilizing power control for direct-drive wind power system. In *Proc. IEEE Power Syst. Technol.*, 1–6.